Geophysical Prospecting, 1980, 28, 872–901.

WAVELET DECONVOLUTION USING A SOURCE SCALING LAW*

A.M. ZIOLKOWSKI,** W.E. LERWILL,***
D.W. MARCH*** and L.G. PEARDON***

ABSTRACT

ZIOLKOWSKI A.M., LERWILL W.E., MARCH D.W. and PEARDON L.G. 1980, Wavelet Deconvolution Using a Source Scaling Law, Geophysical Prospecting 28, 872–901.

We present a new method for the extraction and removal of the source wavelet from the reflection seismogram. In contrast to all other methods currently in use, this one does not demand that there be any mathematically convenient relationship between the phase spectrum of the source wavelet and the phase spectrum of the earth impulse response. Instead, it requires a fundamental change in the field technique such that two different seismograms are now generated from each source-receiver pair: the source and receiver locations stay the same, but the source used to generate one seismogram is a scaled version of the source used to generate the other. A scaling law provides the relationship between the two source signatures and permits the earth impulse response to be extracted from the seismograms without any of the usual assumptions about phase.

We derive the scaling law for point sources in an homogeneous isotropic medium. Next, we describe a method for the solution of the set of three simultaneous equations and test it rigorously using a variety of synthetic data and two types of synthetic source waveform: damped sine waves and non-minimum-phase air gun waveforms. Finally we demonstrate that this method is stable in the presence of noise.

1. INTRODUCTION

The conventional description of a seismic signal regards the propagation of seismic waves as a linear elastic process in which the signal $x(t)$ is obtained as the convolution of the impulse response of the earth $g(t)$ with a far field source wavelet $s(t)$ (Ricker 1940, Robinson 1957, Robinson and Treitel et al.

* Paper read at the 41st meeting of the European Association of Exploration Geophysicists, Hamburg, June 1979, received September 1979.

** National Coal Board; now with The British National Oil Corporation.
*** Seismograph Service (England) Ltd.

 0016-8025/80/1200–8972 $02.00

1973). Usually some additive noise is also present. Thus

$$x(t) = s(t) * g(t) + n(t), \tag{1}$$

where the symbol $*$ denotes convolution. Normally one wishes to extract $g(t)$ uncontaminated by either $s(t)$ or $n(t)$. However, $n(t)$ is not known, and often $s(t)$ cannot be measured or predicted and must also be regarded as unknown.

Since $s(t)$, $g(t)$, and $n(t)$ are all unknowns, the problem of finding $g(t)$ from the measured quantity $x(t)$ is basically that of solving one equation containing three unknowns: it cannot be done, of course. Even when the noise can be ignored the essential difficulty remains: that of deconvolving $s(t)$ and $g(t)$. Unless $s(t)$ is known $g(t)$ cannot be found without making a lot of assumptions.

For more than 20 years much ingenuity has been devoted to devising methods for solving equation (1) using assumptions which are as realistic as possible. But the fact remains that these assumptions are made purely for mathematical convenience. They are not substitutes for hard information.

The best known example of such a method is the least-squares time-domain inverse filtering method (Robinson 1957, Rice 1962) used throughout the industry. For this method to be valid it is required that 1. $g(t)$ be a *stationary*, *white*, *random* sequence of impulses, 2. $s(t)$ be *minimum-phase* and have the *same shape* throughout the seismogram, 3. *there be no absorption.*

All these assumptions are very strong, and they must all be correct *simultaneously* if the method is to work. This condition is very difficult to satisfy, especially since the assumptions are not mutually reinforcing. For example, in attempting to satisfy the stationarity assumption, some sort of spherical divergence correction must first be applied. This has the effect of distorting $s(t)$ unevenly down the seismogram which immediately invalidates the assumption that the shape of $s(t)$ remains constant; it also introduces a tendency for $s(t)$ to be non-minimum phase in the early part of the seismogram.

In this paper we present a method suitable for buried sources, on land and at sea. This method requires none of the assumptions demanded by the other methods. In particular, we assume nothing about differences in the amplitude or phase spectra of $s(t)$ and $g(t)$. We do, nevertheless, begin with the model described by equation (1).

The essential requirement of our method is that the far field source wavelet obeys a scaling law of the type

$$s'(\tau) = \alpha s(\tau/\alpha). \tag{2}$$

In this equation, τ is very nearly equal to $t - r/c$, where t is time measured from the shot instant, r is the distance from the sound source to a point in the

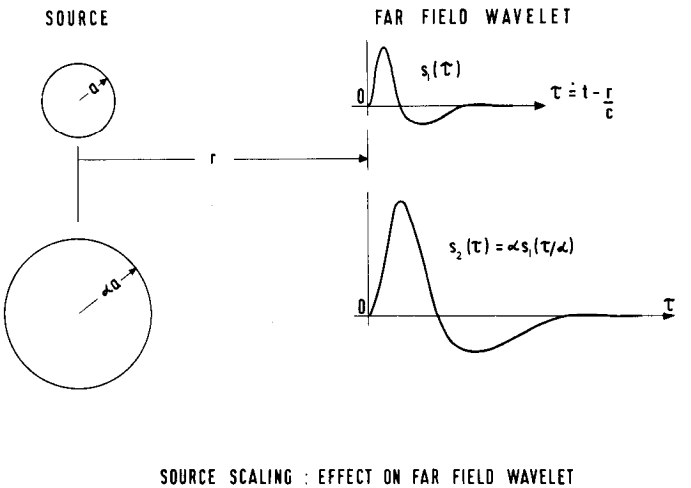

Fig. 1. Effect of source scaling on far field wavelet. As source equivalent cavity is scaled by a factor α, the far field wavelet observed at a distance r scales both in amplitude and delayed time τ by a factor α.

far field, and c is the speed of sound in the medium; $s'(\tau)$ is the far field wavelet of a source similar to that which generates $s(\tau)$, but which contains α^3 times as much energy. Fig. 1 shows how this source scaling law affects the far field wavelet.

There is excellent experimental evidence for the existence of such a scaling law for a variety of point sources, which we shall cite later.

The exploitation of the scaling law is straightforward in principle. We generate a seismic signal $x(t)$ as described by equation (1). We then repeat the experiment *in the same place* using a source of the same type but containing α^3 times as much energy. This will generate the seismogram

$$x'(t) = s'(t) * g(t) + n'(t), \tag{3}$$

where $s'(t)$ is the far field wavelet of the source and is defined in equation (2). $g(t)$ is the same as in equation (1) (because it is the response of the earth to an impulse in the same place); the noise $n'(t)$ may be different from $n(t)$ in equation (1).

Let us consider these equations together for the case where the noise is negligibly small

$$x(t) = s(t) * g(t), \tag{4}$$

$$x'(t) = s'(t) * g(t), \tag{5}$$

$$s'(t) = \alpha s(t/\alpha). \tag{2}$$

In these three independent equations there are three unknowns: $s(t)$, $s'(t)$ and $g(t)$. Therefore, in principle, when the noise is negligibly small, we can solve for all three exactly without making further assumptions.

In the remainder of this paper we put forward a method for the solution of this set of three simultaneous equations, describing all numerical problems we have identified and the techniques we have used to overcome them. We test the method against a variety of synthetic models and show that it is stable in the presence of uncorrelated noise. But first we derive the scaling law for point sources.

2. Derivation of the Scaling Law for a Buried Point Source

We can define a *point source* as one whose maximum dimension is small compared with the shortest wavelength of the useful radiation it generates. If this source is buried in an homogeneous isotropic elastic medium it will generate spherically symmetric radiation at distances greater than about a wavelength. This is the *far field* region in which any aspherical distortions of the wavefield from this point source will occur only at high frequencies outside the useful bandwidth.

In our derivation of the scaling law we require the elastic radiation to have spherical symmetry. The law applies to most marine point sources such as single air guns, single water guns, Maxipulse, Vaporchoc, sparker, etc. On land, it applies to buried explosives, but not to surface sources, because their radiation is not spherically symmetric.

The following derivation is similar to one we gave in an earlier paper (Ziolkowski and Lerwill 1979), but it contains less restrictive assumptions and simpler mathematics. The crux of the argument is the treatment of the nonlinear region close to the source. The argument applied to marine point sources is similar to that for the buried explosive on land except that the medium in which the source is immersed—water—has no rigidity (that is $\mu = 0$).

Consider an explosion in an homogeneous isotropic medium. In the region very close to the explosion the temperatures and pressure immediately after detonation are very high. As the thermal and pressure waves spread away from the detonation their intensities decrease and the medium through which they pass is deformed with a severity which decreases correspondingly: from a melted zone at the center, through zones of crushed, fractured and plastically deformed material, into a zone of elastic deformation. For our purpose there are two distinct regions of deformation: an anelastically deformed one close to the source and an elastically deformed one beyond.

In an earlier paper (Ziolkowski and Lerwill 1979) we assumed that the zone in which the anelastic deformation takes place is spherical. But it is not necessary to assume this in order to derive the scaling law. Since the explosive is a point source for the bandwidth of interest, and therefore exhibits spherical symmetry in the far field, any aspherical distortions in the medium close to the source do not propagate out to the far field—at least not in the bandwidth of interest. The resulting radiation could equally well be generated by a perfectly spherical source which anelastically deforms the same volume of material near to the source and generates the same quantity of elastic radiation: there would be no observable difference between the two sources.

Let the radius of the equivalent sphere of anelastic deformation be a. Let the total available energy stored in the explosive be E, which is proportional to the mass M of the explosive. Thus

$$E = k_1 M, \tag{6}$$

where k_1 is a constant which depends on the chemical composition of the explosive.

We now assume that the fraction β of this energy which is converted into elastic radiation is a constant for a given type of explosive and a given medium. That is

$$E_E = \beta E, \tag{7}$$

where E_E is the energy contained in the elastic radiation. It follows that the energy *not* converted into elastic waves E_A—that is, all the energy absorbed by the sphere of radius a—is given by

$$E_A = (1 - \beta)E. \tag{8}$$

The concentration of energy per unit volume of explosive is much higher than the absorbed energy per unit volume in the anelastic sphere. We may therefore neglect the volume of explosive in relation to the volume of the sphere, provided $(1 - \beta)$ is not *very* much smaller than 1. The capacity of the material to absorb energy is simply proportional to its volume. Therefore

$$E_A = 4k_2\pi a^3/3, \tag{9}$$

where k_2 is a constant which depends on the material. Now, as we have said above, the degree of deformation of the material within the anelastically deformed region varies with the intensity of the thermal and pressure waves. Therefore within this whole region different quantities of energy per unit volume will be absorbed. However, the boundaries between these individual regions are controlled by the limits of temperature and stress which govern

the various modes of energy absorption for the given medium—and these are constant. As more or less energy needs to be absorbed, these individual regions will be *proportionately* larger or smaller, but the number of these regions will remain the same for a given explosive in a given medium. Therefore the total region of anelastic deformation can be considered as a whole for our purpose, and k_2 *is* in fact a constant for a given type of explosive in a given medium.

It follows from equations (6), (8) and (9) that

$$a = KM^{1/3}, \tag{10}$$

where $K^3 = 3k_1(1-\beta)/4\pi k_2$. This equation states that the radius of the equivalent sphere of anelastic deformation is proportional to the cube root of the mass of the explosive.

Outside this sphere we have elastic radiation. This radiation could be obtained equally well by replacing the sphere with a cavity of radius a at the interior of which we apply a time-dependent pressure function $P(t)$. This pressure function is unknown, but exactly equal to the incident pressure wave at a distance a from the detonation which produces the observed radiation. The reason for using this argument is that the problem of the generation of elastic waves by a spherical cavity in an homogeneous isotropic elastic medium has been solved (Sharpe 1942, Blake 1952).

Sharpe (1942) considered the case where the Lamé constants λ and μ of the medium are equal. Blake (1952) solved the same problem for arbitrary λ and μ. Using either solution the far field signature (either in displacement u, particle velocity $\dot{u}$, or pressure $p = \rho c\dot{u}$, where ρ is density and c is velocity of sound) can be calculated for any given pressure function $P(t)$ applied at the interior of the cavity. For example, Sharpe (1942) gives the far field displacement for

$$P(t) = \begin{cases} p_0, & t > 0 \\ 0, & t < 0 \end{cases} \quad \text{as:}$$

$$u(\tau) = \frac{a^2 p_0}{2\sqrt{2}\,\mu r} \exp\left(\frac{-y\tau}{\sqrt{2}}\right) \sin(y\tau), \tag{11}$$

where $\tau = t - (r-a)/c$ and $y = 2\sqrt{2}\,c/3a$. The particle velocity is obtained by differentiating equation (11) with respect to time to yield

$$\dot{u}(\tau) = \frac{ap_0 q}{2\sqrt{2}\,\mu r} \exp\left(\frac{-q}{\sqrt{2}}\frac{\tau}{a}\right)\left[\cos\left(q\frac{\tau}{a}\right) - \frac{1}{\sqrt{2}}\sin\left(q\frac{\tau}{a}\right)\right], \tag{12}$$

where we have put $q = ay = 2\sqrt{2}\,c/3$. We recognize now that the far field particle velocity function can be written in the form

$$\dot{u}(\tau) = p_0 \frac{a}{r} f_s(\tau/a). \tag{13}$$

For any given pressure function $P(t)$ at the interior of the cavity we can find $\dot{u}(\tau)$ in the far field using equation (13) and Duhamel's integral:

$$\dot{u}(\tau) = \frac{a}{r} \frac{\mathrm{d}}{\mathrm{d}t} \int_0^\tau P(n) f_s\left(\frac{\tau - n}{a}\right) \mathrm{d}n \tag{14}$$

(an expression of the same form would have been derived if we had started with Blake's (1952) solution).

Equation (14) contains the unknown function $P(t)$. In order to proceed any further we must make some sort of assumption about $P(t)$. *The most satisfactory and least restrictive assumption that we have been able to find is that, whatever the exact form of $P(t)$, it is independent of the mass M of the explosive and is constant for explosives of the same chemical composition in the same medium.* If this is true we note that $\dot{u}(\tau)$ has the simpler form

$$\dot{u}(\tau) = \frac{a}{r} f(\tau/a), \tag{15}$$

where f is constrained, by energy considerations, to satisfy the following expression (appendix C):

$$\int_0^\infty f^2(\eta)\, \mathrm{d}\eta = \frac{\beta k_2}{3(1-\beta)\rho c}. \tag{16}$$

The right-hand side contains only constants which depend on the medium and type of explosive. Thus f is *inherently* a function of these two factors and is independent of the mass of the explosive. The far field pressure function is easily derived from $\dot{u}$, as we have noted ($p = \rho c \dot{u}$). The variable (τ/a) is scaled time measured from the instant of arrival of the wavelet at a distance r from the center of detonation.

We now have everything we need to derive the scaling law. Consider two explosives of masses M_1 and M_2, with equivalent cavities of radii a_1 and a_2, and far field particle velocity functions $\dot{u}_1$ and $\dot{u}_2$, respectively:

$$\dot{u}_1(\tau_1) = \frac{a_1}{r} f\left(\frac{\tau_1}{a_1}\right), \tag{17}$$

$$\dot{u}_2(\tau_2) = \frac{a_2}{r} f\left(\frac{\tau_2}{a_2}\right), \tag{18}$$

where $\tau_1 = t - (r - a_1)/c$ and $\tau_2 = t - (r - a_2)/c$. If we let the ratio of M_2/M_1 equal α^3, it follows from substitutions into equation (10) that

$$a_2 = \alpha a_1. \tag{19}$$

If we make the approximation

$$\tau_2 = \tau_1 = \tau, \tag{20}$$

we find from equations (17), (18) and (19) that

$$\dot{u}_2(\tau) = \alpha \dot{u}_1(\tau/\alpha), \tag{21}$$

which is our scaling law. Since $p = \rho c \dot{u}$ in the far field, we can find an expression similar to equation (21) for $p(\tau)$. In general, this equation for the scaling of the far field source wavelet can be written as

$$s'(\tau) = \alpha s(\tau/\alpha), \tag{22}$$

where $s(\tau)$ and $s'(\tau)$ are the two far field wavelets (both either particle velocity or pressure functions) and α is the scale factor equal to the cube root of the corresponding ratio of the source masses or source energies. The approximation given by equation (20) is sufficiently accurate if the time interval $\Delta\tau = (a_1 - a_2)/c$ is unobservable within the frequency band of interest; that is, $\Delta\tau$ should be less than about one sample interval. This approximation will probably hold for values of α up to about 5 or so.

The scaling law of equation (22) is very well known. It implies that both the amplitude and period of far field source wavelets will scale as the cube root of the mass or the energy of the charge. O'Brien (1969) found that this law held for both primary compressional (P) and shear (S) waves for charge weights varying from 0.08 to 9.5 kg. However, O'Brien also found that the larger charges were "more efficient generators of seismic energy"—that is, a larger fraction of the initial available energy is converted into elastic radiation by larger charges. In the above derivation we required the efficiency of generation of seismic energy to be *independent* of charge size in order to find the scaling law. Indeed in our earlier paper (Ziolkowski and Lerwill 1979) we show in appendix B that the seismic efficiencies must be identical if the scaling law is true. It is not clear how the discrepancy between these observations arises.

Using measurements of displacement, rather than of particle velocity or pressure, Frasier and North (1978) show that the corresponding scaling law gives a very good fit to large U.S. explosions in the magnitude (m_b) range 3.4–6.2 for short period *P*-waves in the period range 0.5 s to more than 1.5 s.

The evidence for the applicability of the scaling law to buried explosives on land is thus very good. At sea, where the medium is far more homogen-

eous and isotropic, the law should apply even more exactly. In fact the law is accepted for air gun waveforms and is used in the design of air gun arrays (Nooteboom 1978).

It should be remembered that many factors contribute to the shape of the far field wavelet, including the depth of the charge. We have considered the effect on the wavelet of only *one* parameter: the charge mass. To relate this to other sources, one must consider changing only the mass of the source. For an air gun, for example, the depth and pressure of the gun must be the same, but the volume may change.

Finally, we note that the theory as presented applies only to *point* sources. In practice, however, *arrays* of sound sources are used, particularly in the marine environment. Arrays normally generate radiation which is not spherically symmetric and consequently the basic assumption of the theory is violated. However, by utilizing a simple design procedure for the array configuration the theory can be extended to this field. This is the subject of a separate paper by A. Ziolkowski.

3. Solution of the Equations in the Frequency Domain

When we first considered this problem we found that by transforming the equations to the frequency domain we were able to separate the variables very easily. A simple algorithm presented itself and, at first sight, yielded the Fourier transform of the source wavelet without difficulty. However, there are several important considerations to be taken into account, as we have found with some effort (more enlightened students would doubtless have found the same with less trouble). Thus, even though we are not convinced that we have the most efficient scheme, there are several interesting aspects of it which are worth discussing—if only because they may have applications in other areas.

(a) *The basic scheme*

In the absence of noise the equations we are required to solve are

$$x(t) = s(t) * g(t), \tag{4}$$

$$x'(t) = s'(t) * g(t), \tag{5}$$

$$s'(t) = \alpha s(t/\alpha). \tag{2}$$

Taking the Fourier transforms of these equations we have

$$X(f) = S(f) \cdot G(f), \tag{23}$$

$$X'(f) = S'(f) \cdot G(f), \tag{24}$$

$$S'(f) = \alpha^2 S(\alpha f). \tag{25}$$

Dividing equation (24) by equation (23) and substituting for $S'(f)$ from equation (25) we find

$$\frac{X'(f)}{X(f)} = R(f) = \frac{\alpha^2 S(\alpha f)}{S(f)}. \tag{26}$$

Therefore

$$S(\alpha f) = \frac{1}{\alpha^2} S(f) \cdot R(f). \tag{27}$$

Equation (27) suggests a recursive algorithm of the form

$$S(\alpha^n f_0) = \frac{1}{\alpha^2} S(\alpha^{n-1} f_0) R(\alpha^{n-1} f_0), \tag{28}$$

$$n = 1, 2, \ldots, N,$$

where N is dictated by the highest frequency of interest, and the process must be initiated with a guess at f_0. If $\alpha > 1$ equation (28) enables us to work up the spectrum calculating values at $\alpha f_0, \alpha^2 f_0, \ldots, \alpha^N f_0$, starting with a guess at f_0.

To compute values at frequencies *less* than f_0, equation (27) can be re-arranged

$$S(f) = \alpha^2 S(\alpha f)/R(f),$$

such that we obtain the recursion

$$S(f_0/\alpha^n) = \alpha^2 S(f_0/\alpha^{n-1})/R(f_0/\alpha^n), \tag{29}$$

$$n = 1, 2, \ldots, M,$$

where M is dictated by the lowest frequency of interest. This now enables the values at frequencies $f_0/\alpha, f_0/\alpha^2, \ldots, f_0/\alpha^M$, to be computed.

Thus from the recursion scheme of equations (28) and (29) we can obtain values at frequencies $f_0/\alpha^M, f_0/\alpha^{M-1}, \ldots, f_0/\alpha, f_0, \alpha f_0, \ldots, \alpha^N f_0$.

We can now use an interpolation routine to find a value at another specified frequency, say f_1, and use the recursion to calculate values at αf_1, $\alpha^2 f_1$, etc. This procedure is repeated until sufficient values have been

computed. Once $S(f)$ has been calculated, $s(t)$ is obtained by taking the inverse Fourier transform.

It should be noted that the quantities involved in the algorithm are complex. One can operate either with the modulus (amplitude) and argument (phase), or with the real and imaginary parts. We have used the real and imaginary parts in all our examples as we feel that these are the most "basic" components of the complex numbers in a computer, whereas amplitude and phase are derived from these quantities.

(b) *The initial guess*

The algorithm is initiated with a guess. If this guess is wrong, the final result will be wrong. The guess at f_0 is a complex number which, in all probability, will not be the true value at f_0. In fact, the guess $S_G(f_0)$ is related to the true value $S(f_0)$ in the following way

$$S_G(f_0) = re^{i\theta} S(f_0), \tag{30}$$

where $re^{i\theta}$ is the unknown complex error factor. If we fail to take this error into account we generate the values

$$S_G(\alpha^n f_0) = \frac{1}{\alpha^2} S_G(\alpha^{n-1} f_0) \cdot R(\alpha^{n-1} f_0), \tag{31}$$

$$n = 1, 2, \ldots, N$$

which, with sufficient interpolation, yields the function $S_G(f)$ for $f_0/\alpha^M \leq f \leq \alpha^N f_0$. The range can be extended to the origin by defining $S_G(0) = 0$ which is compatible with a time series $s_G(t)$ with zero mean.

The effect of our initial error can be seen by substituting for $S_G(f_0)$ from equation (30) into equation (31):

$$S_G(\alpha^n f_0) = re^{i\theta} S(\alpha^n f_0) = \frac{1}{\alpha^2} re^{i\theta} S(\alpha^{n-1} f_0) \cdot R(\alpha^{n-1} f_0). \tag{32}$$

It is evident that the error factor is constant for all values deduced from the algorithm. Thus far the algorithm has allowed us to compute the function

$$S_G(f) = re^{i\theta} S(f), \qquad (0 \leq f \leq \alpha^N f_0), \tag{33}$$

where we have asumed f_0 to be positive.

We are now faced with two problems. First we must complete our transform by generating values of $S_G(f)$ at negative frequencies. Secondly, we must find our error factor to obtain $S(f)$ from equation (33). We can solve both these problems by consideration of the physical properties of $s(t)$, which impose constraints on the properties of $S(f)$.

We know that $s(t)$ is *real*, and therefore our estimated wavelet should be real. This constraint imposes Hermitian symmetry on $S(f)$. That is, the real and imaginary parts of $S(f)$ must be even and odd functions, respectively. Thus, if we know $S(f)$ for positive frequencies, we can easily compute $S(f)$ for negative frequencies using this condition.

However, we only know $S_G(f)$, which is in error by a phase shift θ and a scale factor r. The scale factor is unimportant because it has no effect on the *shape* of $s(t)$, and consequently cannot affect our estimate of the shape of $g(t)$. We can therefore ignore it. But we cannot ignore the phase error θ, because this will make $s_G(t)$ non-causal, and we know that $s(t)$ is causal, that is, $s(t)$ is zero for negative times t. In the frequency domain causality imposes the condition that the odd and even parts of the Fourier transform are a Hilbert transform pair (Bracewell 1965, pp. 271–2). It can be shown that this causal relationship is destroyed unless the phase error θ is zero (see appendix A).

This consideration suggests a trial-and-error procedure for improving our estimate of $s(t)$. This is as follows:

1. Compute $S_G(f)$ from an initial guess at f_0 as described above, noting that $S_G(f)$ and $S(f)$ are related as in equation (33).
2. Multiply $S_G(f)$ by a correction factor $e^{-i\theta_G}$ where θ_G is a guess.
3. Impose Hermitian symmetry.
4. Check for causality. If the recovered wavelet is non-causal, return to step (2) and repeat, using a different θ_G. This procedure is repeated until the causality condition is met.

Thus the equations may be solved in the frequency domain using the algorithm described above and applying the constraints which follow from two physical properties of $s(t)$: it is *real* and *causal*. Our final estimate of $s(t)$ will be in error only by a scaling factor r, which is trivial. Having obtained a satisfactory estimate of $s(t)$ we can obtain $g(t)$ using equation (1) by standard methods.

In applying the above scheme to solve for $S(f)$ in the absence of noise, we come across two numerical problems associated with the complex ratio. These can be dealt with quite simply, as discussed in the following section.

(c) *The complex ratio*

The algorithm we have described depends on a complex division in the frequency domain. There are two problems associated with this. First, the ratio becomes unstable at any frequency at which the amplitude of the denominator is too small. Secondly, if the denominator contains non-minimum-phase components which are not contained in the numerator then

the quotient becomes unstable in the sense that it is non-realizable (Robinson 1967).

To solve the first problem it is usual to add a small threshold of white noise to the denominator to negate the possibility of zero or near zero division. An alternative—but more time-consuming—method is to search for low values in the denominator and to replace them with small positive values.

Finding the inverse of non-minimum-phase wavelets is a well-known problem (Robinson 1967). However, since we are dealing with a ratio, we can avoid the problem simply by applying an exponential taper of the form $e^{-\gamma t}$ to both $s(t)$ and $x'(t)$. By choosing γ large enough we can force the quotient $R(f)$ to be stable, but then our estimates of $s(t)$, $s'(t)$, and $g(t)$ will be distorted. In practice we may remove the distortion simply by applying the inverse taper $e^{\gamma t}$ to these functions. (Schafer 1969).

(d) *The Presence of Noise*

In the presence of noise the problem is to obtain a reliable estimate of the ratio spectrum $R(f)$, for then the scaling law and recursive algorithm can be used to find $S(f)$ as described above.

From equation (26) we define $R(f)$ in the absence of noise as

$$R(f) = \frac{X'(f)}{X(f)} = \frac{S'(f)}{S(f)}. \tag{26}$$

It follows that

$$s'(t) = r(t) * s(t), \tag{34}$$

where $r(t)$ is the inverse Fourier transform of $R(f)$ and, since $s(t)$ and $s'(t)$ are both real and causal, $r(t)$ must also be real and, if $s(t)$ is minimum phase, causal. In the noise-free case it is then true that

$$x'(t) = r(t) * x(t), \tag{35}$$

and we see that $r(t)$ is simply a one-sided filter which shapes $x(t)$ into $x'(t)$.

When noise is present we have to stabilize our estimate of $r(t)$. This can easily be done using the Wiener-Levinson (1947) least-squares approach. That is, we find a filter $r'(t)$ which, for an input $x(t)$, gives an output which is the best fit in a least-squares sense to $x'(t)$. This filter $r'(t)$ is our best estimate of $r(t)$.

In other words, in the presence of noise we can calculate $r(t)$ in the time domain using standard programmes, and then take its Fourier transform and proceed from there to find $S(f)$, $s(t)$, etc., as described above. It should be noted that when we have multichannel recording we can make a number of

independent estimates of $r(t)$ for each pair of shots. We can combine these estimates to improve the signal-to-noise ratio.

4. Solution of the Equations in the Time Domain

The scheme outlined above does not yield a solution directly: it is necessary to converge on it by use of the trial-and-error procedure described in 3(b). This is not especially convenient, and we therefore considered the possibility of arriving at a solution more directly in the time domain. An obvious method presented itself (see appendix B), but it suffers from apparent numerical instability. It may well be possible to solve the equations in the time domain without incurring this penalty by using some other method. We have not investigated this further.

A more elegant solution to this problem was offered by Mr R. Calvert of Shell (U.K.) Limited, who worked it out one evening immediately after the presentation of this paper in Hamburg. His solution is presented in appendix D.

All the examples which we present in the next section were calculated using the scheme described in section 3 above.

5. Examples

(i) Our first example was chosen simply to test our computer program in the absence of noise. We chose as our basic wavelet a damped sine wave shown as s_1 in fig. 2. We then constructed a scaled version of this, choosing $\alpha = 2$ (s_2 in fig. 2). We then treated s_1 and s_2 as our two seismograms $x(t)$ and $x'(t)$—that is, the reflectivity series $g(t)$ is a delta-function at time $t = 0$. Using our three simultaneous equations, we recovered the basic wavelet as shown in the figure. The reflectivity series was recovered in the frequency domain by dividing the Fourier transform of s_1 by the Fourier transform of the recovered wavelet. The result is shown at the bottom of fig. 2.

It will be noted that the recovered wavelet is very similar to the original. The reflectivity series should be a perfect spike, but is slightly noisy. The noise is predominantly in the high frequencies where there is very little energy in the original data. Clearly, the more narrow band the basic wavelet is, the more noise is generated outside this band in the reflectivity series. Noise outside the signal band can be filtered out in the normal way.

(ii) For our second example we wanted to test the scaling law for realistic data, and at this stage we wished to exclude the problems introduced by noise. We therefore chose to use synthetic waveforms generated independently of the scaling law.

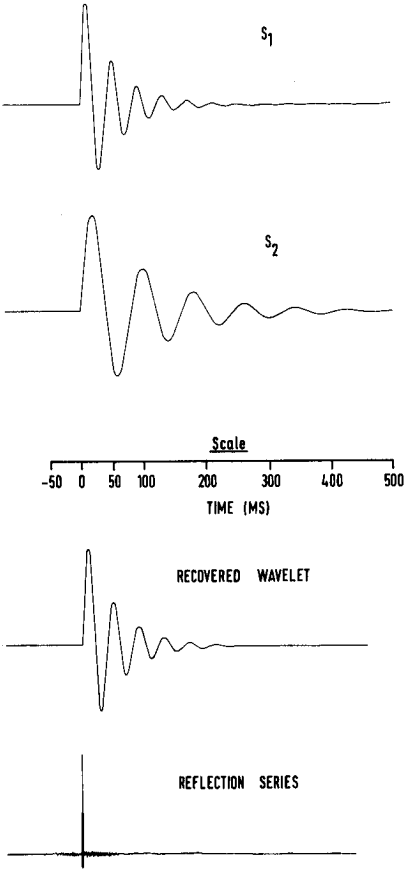

Fig. 2. Demonstration that proposed solution works on a damped sine wave. The wavelet s_1 is a damped sine wave; s_2 is a scaled version of s_1 in which α equals 2; the recovered wavelet and reflection series have been obtained from s_1 and s_2 assuming these are observed seismograms. *All wavelets from figs 2–8 have been normalized to make maximum amplitudes equal.*

The model we used to generate our waveforms was discussed by Ziolkowski (1970) and is based on the nonlinear oscillations of a spherical bubble in water. The waveforms generated by the model closely resemble those of airguns without wave-shape kits (Ziolkowski 1970, 1971, Smith 1975). The advantage of this model is that it is essentially nonlinear in the region close to the bubble wall and therefore provides a severe test of our treatment of the scaling of the anelastic region close to the source. Furthermore, the waveform produced by the model is not minimum-phase (Ziolkowski 1971) and, because it closely resembles the waveform produced by an airgun, it will give a good indication of the performance of this technique on real data generated

(with air guns—especially since real air gun waveforms are also non-minimum-phase (Berkhout 1970, Ziolkowski 1971).

We generated two independent far field source wavelets using this model, as shown in fig. 3. The first wavelet was computed for a 0.164 l (10 cubic inch) gun at a depth of 9.15 m (30 feet), a firing pressure of 13.7 MPa (2000 psi) and a range of 150 m (500 feet) from the gun. No sea surface reflection has been included. The second wavelet was computed using the same computer program for a 1.3 l (80 cubic inch) gun, at the same depth, firing pressure and range. In other words, only the volume was changed.

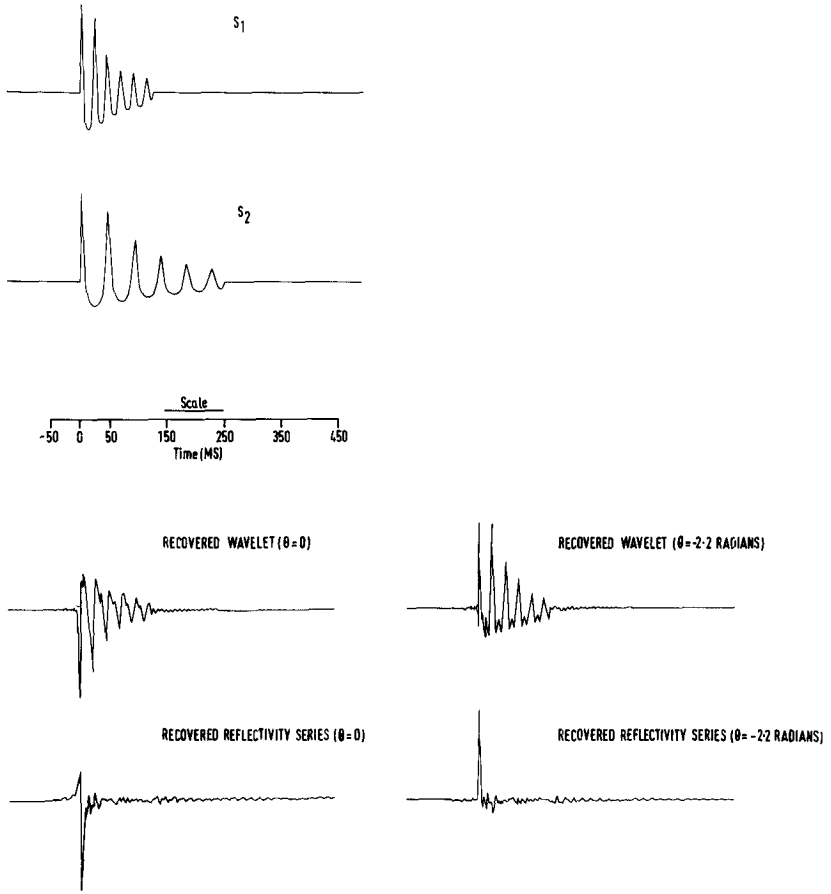

Fig. 3. Effect of errors in initial guess at f_0. The wavelet s_1 is a theoretical wavelet, without a ghost, from a 0.164 l (10 cu. in.) air gun at a depth of 9.15 m (30 ft) and pressure of 136 bar (2000 psig); s_2 is a theoretical wavelet, without a ghost, from a 1.312 l (80 cu. in.) gun at a depth of 9.15 m and pressure of 13.7 MPa. With initial guess ($\theta = 0$) the recovered wavelet and reflectivity series are shown on bottom left with reflectivity series distinctly non-causal. Correcting by -2.2 radians yields a better recovered wavelet and causal reflectivity series as shown on bottom right.

Using the scheme described above—and without making any compensations for the mixed-phase property of the basic wavelet or for the error (in phase) in our initial guess of $S(f_0)$ we recovered the wavelet shown in fig. 3. The recovered reflectivity series, which should be a spike at time $t = 0$, is non-causal and noisy.

We found that it was essential for the recovery of a satisfactory wavelet to correct for both the mixed-phase property of the wavelet and the error in our initial guess to ensure that the recovered wavelet and reflectivity series are causal—as described above in section 3.

The causality constraint is best satisfied in this case with a phase correction of $\theta = -2.2$ radians. The result of this correction is shown on the right of fig. 3, where the recovered wavelet and reflectivity are now both causal, but still noisy. This noise is introduced by failing to compensate for the mixed-phase character of the basic wavelet. We therefore applied an exponential taper of the form $e^{-\gamma n \Delta t}$ to both s_1 and s_2, where $e^{-\gamma \Delta t}$ was equal to 0.994. The result of this damping is shown in the first two wavelets of fig. 4. The recovered wavelet, corrected for the error in our initial guess, is shown; no inverse tapering has been applied. The corresponding unfiltered recovered reflectivity series and the original, undamped, wavelet are also shown. Both the wavelet and recovered reflectivity series are acceptable. Some zero-phase low-pass filtering has been applied to the recovered wavelet. The lack of high frequency energy in the wavelet has caused extra noise to appear in the recovered reflectivity series. This can be removed by low-pass filtering in the normal way.

(iii) The first two examples show that the scheme we have described works even when the basic wavelet has a complicated shape and is not minimum-phase. We now show that it is possible to recover a complicated reflectivity series.

We took the same two wavelets, shown at the top of fig. 3, and convolved them with the synthetic reflectivity series shown at the top of fig. 5. We then applied the same exponential tapering, with the result shown as the next two time series on the left of fig. 5. Using the same trial-and-error correction to ensure causality, we recovered the basic wavelet and reflectivity series shown at the bottom of the figure. To both the recovered wavelet and recovered reflectivity series a small amount of zero-phase bandpass filtering was applied to remove high frequency noise. The recovered wavelet very closely resembles a damped version of the original (shown on the right of the figure) while the recovered reflectivity series, which has had inverse damping applied, preserves the times and relative amplitudes of the reflection exactly—as one would expect from the theory.

It should be noted that no ghost has been included. If a ghost had been

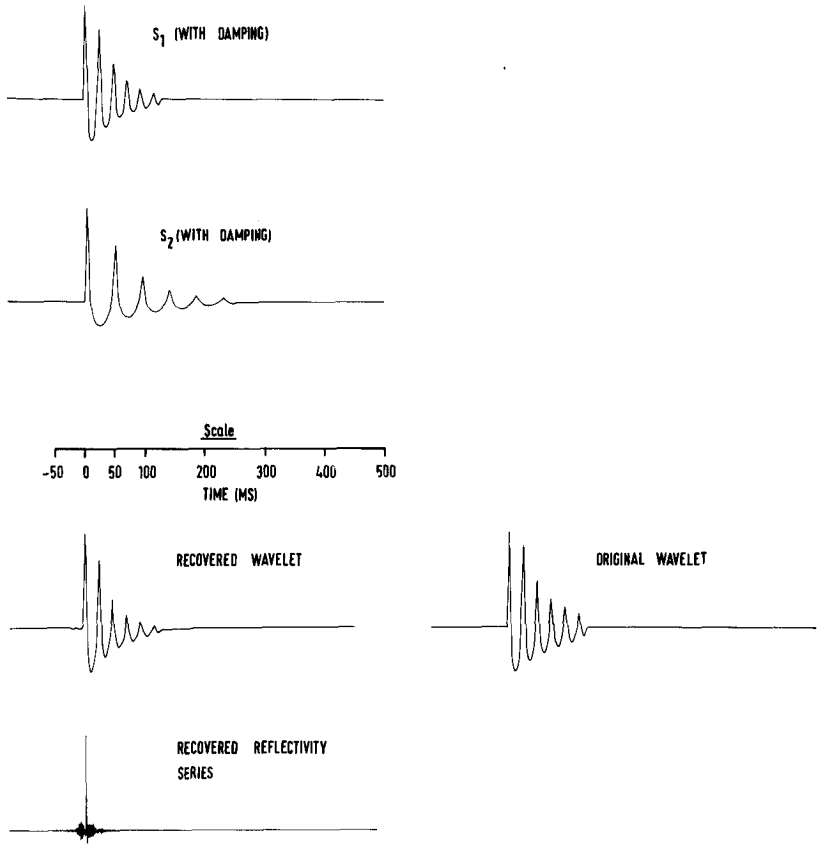

Fig. 4. Showing effect of non-minimum phase wavelet. The wavelets s_1 and s_2 are identical with those in figure 3, but have been damped with exp $(-\gamma n\ \Delta t)$ where exp $(-\gamma\ \Delta t) = 0.994$. Using the same correction factor for the initial guess ($\theta = -2.2$ radians), the recovered wavelet (with*out* inverse damping) and the recovered reflectivity series (*with* inverse damping) are as shown. The original undamped wavelet is also shown for comparison.

included, the recovered wavelet would be the same. However, each spike in the recovered reflectivity series would now be followed by a second spike of opposite polarity at the ghost delay. In other words, the recovered series would be equal to the original reflectivity series convolved with a two-point operator corresponding to the arrival of the direct wave and the ghost.

(iv) All the above examples were computed entirely in the frequency domain. However, as we suggested in section 3(d), whenever noise is present the spectral ratios which are needed for this approach should be calculated in the time domain using Wiener filters. We note that in the absence of noise this process will not be quite so accurate, but in the real world noise is always

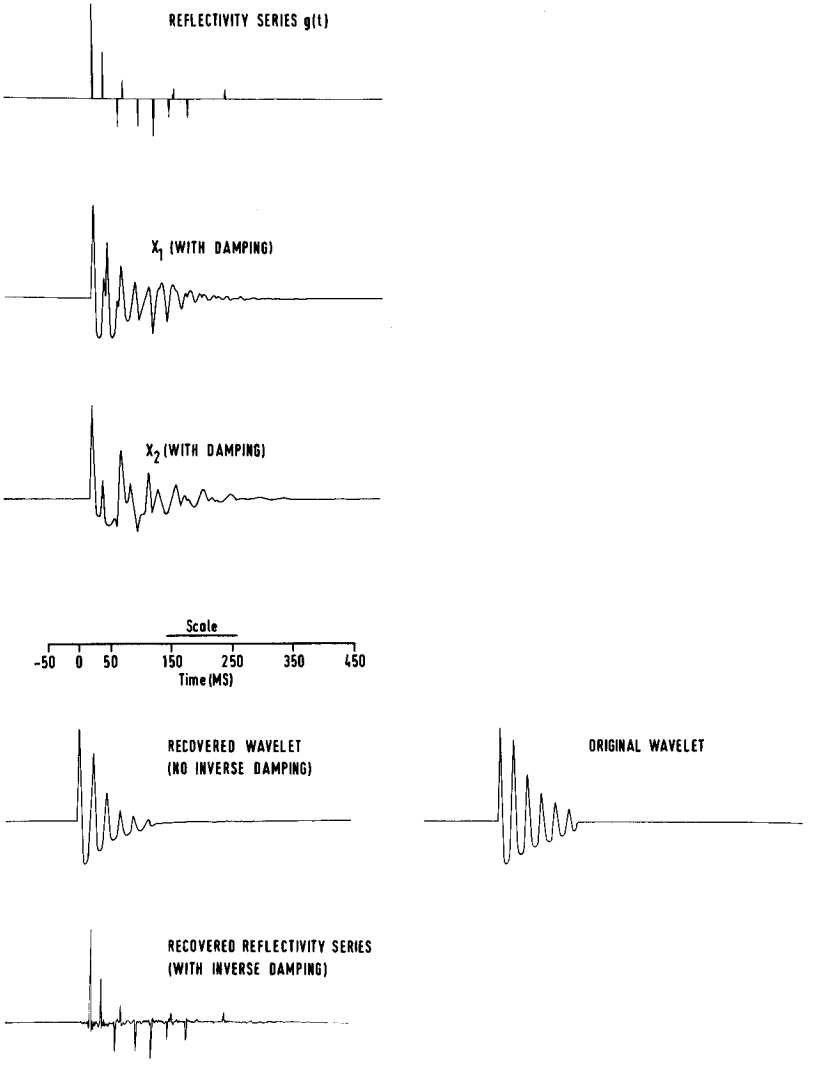

Fig. 5. Effect of synthetic geology on wavelet recovery in the absence of noise: $g(t)$ is reflectivity series; x_1 and x_2 are the results of convolving $g(t)$ with the wavelets s_1 and s_2 of fig. 3 and then applying exponential damping. The recovered wavelet and reflectivity sequence are shown below. The original undamped wavelet is shown for comparison.

present to some degree. In this next example we added non-correlated Gaussian noise to the basic wavelets shown at the top of fig. 3. The result is shown in fig. 6. Using the modified approach of section 3(d) and with the appropriate weighting and correction factor we recovered the wavelet and the spike shown at the bottom of the figure. Since the noise is additive we found it

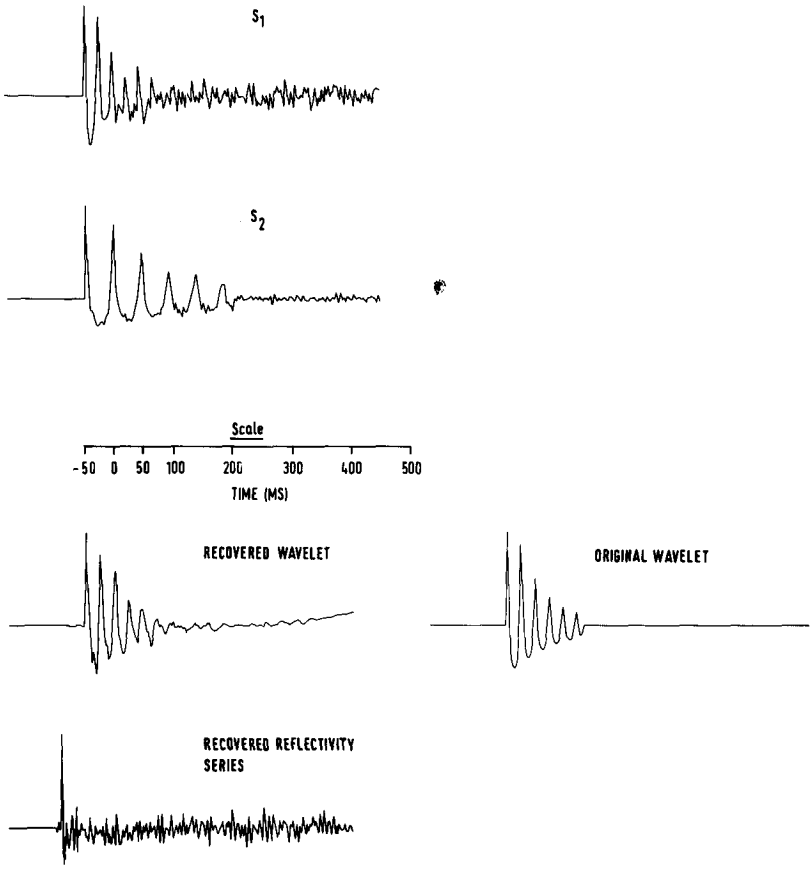

Fig. 6. Stability of calculation in the presence of noise. The wavelets s_1 and s_2 are the same as those shown in fig. 3, but non-correlated noise with the same bandwidth as the signal has been added to each—at the same level. A stable wavelet is recovered for a signal to noise ratio of about 4 (rms), the inverse damping revealing a slight very low frequency component. The noise appears on the recovered reflectivity series of course.

desirable to "unweight" the recovered wavelet and original signal prior to extraction of the reflectivity series.

The calculation is clearly stable in the presence of this type of noise and we have shown this to be true for signal-to-noise ratios down to 4 : 1 (rms). As the signal-to-noise ratio decreases there is a progressive loss of accuracy in the recovery of the wavelet as one might expect.

We have repeated this test using the same synthetic reflectivity series of fig. 5 and adding the same noise that we used for the example shown in fig. 6. The result is shown in fig. 7, where our claims for the stability of the process remain as firm. The recovery of the wavelet is still quite good. The recovery of

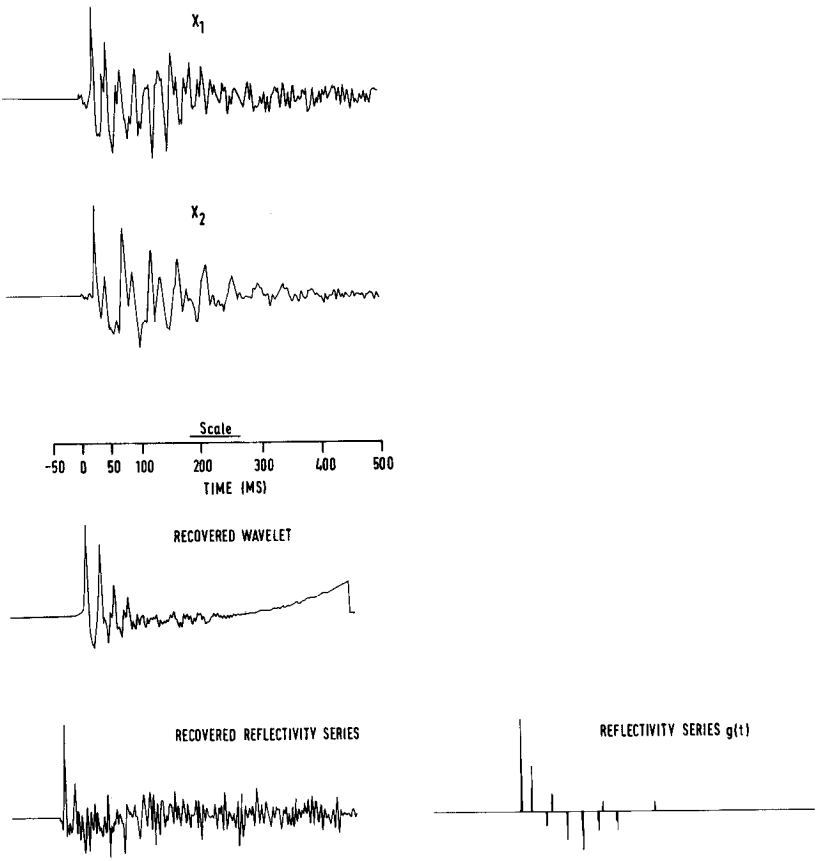

Fig. 7. Showing effect of synthetic geology and noise. x_1 and x_2 are the undamped synthetic seismograms of fig. 5 with noise added. A stable recognizable wavelet is recovered with a small very low frequency component. The recovered reflectivity series is noisy compared with the synthetic.

the reflectivity series is good for signal-to-noise *amplitude* ratios of 3 : 1 or better and is still reasonable down to 2 : 1. Signal-to-noise ratio limitations are common to all wavelet extraction processes and various methods are employed to bring about improvements. In our case the signal-to-noise ratio can be improved by compositing within a two-record pair as mentioned above in section 3(d).

(v) Finally, we have an example to show that there is a real improvement over conventional deconvolution when the wavelet is non-minimum phase, or when the reflectivity series is non-white or non-stationary. Using a Wiener filter we attempted to recover the reflectivity series from the noise-free seismogram shown at the top of fig. 5. The result is shown in fig. 8.

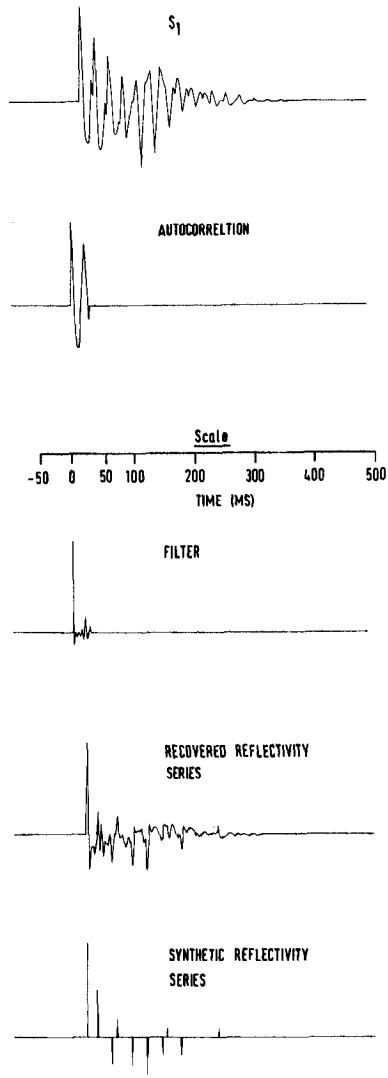

Fig. 8. The application of standard least-squares deconvolution to the noise-free sequence x_1 shown in fig. 5. The one-sided truncated autocorrelation of x_1 is shown, followed by the spiking deconvolution filter and the resulting reflectivity series. The original synthetic is shown below for comparison.

For theoretical reasons we would expect this least-squares inverse filtering approach to fail, as discussed in section 1. It is interesting to note just *how* it fails. First, the relative amplitudes of the individual events are incorrect, even though the method does find events at the correct times. Secondly, it also finds events at incorrect times—and this is a form of noise.

In such situations, where conventional wavelet extraction methods fail because the mathematical assumptions on which they are based are incorrect, our approach should yield more accurate results, with correct relative amplitudes of reflections, and with a superior signal-to-noise ratio.

6. Conclusions and Qualifications

We have presented a new approach for the extraction and removal of the source wavelet from the seismogram. It requires a fundamental change in the field technique such that two different seismograms are generated for each source-receiver pair. A well-known scaling law provides the relationship between the two source signatures.

The convolutional earth model of the two seismograms plus the scaling law together constitute three simultaneous equations which can, in principle, be solved exactly in the absence of noise. In practice, a small amount of noise is introduced when the data are band-limited. The method of solution which we have proposed here is stable in the presence of noise, indicating that the method will work with real data.

The principal advantage of this deconvolution method over all the other methods currently in use is that this one does not demand that there be any mathematically-convenient relationship between the phase spectrum of the source and the phase spectrum of the earth impulse response. Our method can be applied when, for example, (a) the phase spectrum of the source is non-minimum phase and (b) the impulse response of the earth is neither white nor stationary. In such situations conventional methods are likely to introduce spurious reflections—a form of noise—and fail to yield the correct relative amplitudes of real reflections. This fault is not shared by our method.

This point is particularly important when seismic data are processed for the interpretation of lithological changes via derived acoustic impedance logs. The first step in this processing sequence is the recovery of the impulse response of the earth by removal of the source far field wavelet. If this step is wrong, all subsequent steps will not be able to correct for this original error. Unless the source wavelet shape is *known*, it is not possible to recover the earth impulse response. Unless the source wavelet is measured, it can only be recovered from the data, using conventional techniques, if a number of essential assumptions happen to be true simultaneously. Our approach permits these assumptions to be avoided, and still allows the earth impulse response to be recovered even though the source wavelet is not measured. Subsequent recovery of the primary reflectivity sequence by standard processes may then follow.

We do have one qualification to make about our approach concerning

the effects of absorption. All other deconvolution techniques neglect the effect of absorption over the window of interest. In our method all calculations refer to the shot instant, time $t = 0$. If absorption is convolutional it simply appears as part of the earth impulse response $g(t)$ and does not affect the accuracy of the theory. If it is *not* convolutional and is not even closely approximated by a convolutional model, then our method will fail. This is because the effect of absorption will not divide out when we form our spectral ratio $R(f)$. Thus $R(f)$ will not closely approximate $S'(f)/S(f)$, as we require. This is a problem of which we are well aware. However, we have not done any fundamental research to determine whether absorption can be closely approximated by a convolutional model as we have assumed.

We see non-convolutional absorption as an obstacle to the success of our technique. However, if absorption *is* largely convolutional it is no obstacle at all. The technique has many advantages over the other existing methods and, in our view, replaces mathematical assumptions of dubious validity by well-known physical laws.

ACKNOWLEDGMENTS

We have benefited from numerous discussions with many friends and colleagues.

We would like to thank the following friends in particular: Clint Frasier for his help in understanding source scaling; John Mahoney for pointing out that $f(\tau/a)$ in equation (15) is not an unconstrained function of (τ/a); Elio Poggiagliolmi for suggesting the use of a Wiener filter to estimate $r(t)$ in equation (35); R. Calvert for proposing the solution reproduced here as Appendix D; and all the members of Seismograph Service (England) Limited Research Department for provocative discussions and helpful suggestions. We are especially grateful to Mrs J.H. Plaister and Ms. S. de Rozario for typing drafts, "final" manuscripts and "final final" manuscripts.

We thank the National Coal Board and the Directors of Seismograph Service (England) Limited for permission to publish this paper.

The views expressed here are our own and are not necessarily those of the National Coal Board.

APPENDIX A

The algorithm described in section 3 yielded the one-sided function given by equation (33)

$$S_G(f) = re^{i\theta}S(f), \qquad 0 \leq f \leq \alpha^N f_0 . \tag{A1}$$

This was extended to negative frequencies by imposing Hermitian symmetry, and it was asserted that this resulted in the recovered wavelet being non-causal, unless the phase angle θ were zero. This will now be proved.

Proof

We first assume that truncation effects are negligible so that equation (A1) can be regarded as valid for $0 \leq f < \infty$. After applying Hermitian symmetry we obtain the function

$$S_G(f) = re^{i\theta}S(f)U(f) + re^{-i\theta}S^*(-f)U(-f), \tag{A2}$$

where $U(f) = 1$ for f positive, $=0$ otherwise, and S^* is the complex conjugate of S.

Equation (A2) can be written as

$$S_G(f) = S(f)re^{i\theta \operatorname{sgn} f} \quad \text{for all } f, \tag{A3}$$

where

$$\operatorname{sgn} f = 1, f > 0; \; = -1, f < 0.$$

Now

$$re^{i\theta \operatorname{sgn} f} = r\cos(\theta \operatorname{sgn} f) + ir\sin(\theta \operatorname{sgn} f) = r(\cos\theta + i \operatorname{sgn} f \sin\theta). \tag{A4}$$

If we put $a = r\cos\theta$ and $b = r\sin\theta$, and substitute from equation (A4) into equation (A3), we find

$$S_G(f) = S(f) \cdot [a + ib \operatorname{sgn} f]. \tag{A5}$$

In this equation $S(f)$ is the Fourier transform of the original real causal wavelet $s(t)$, and i sgn f is the Fourier transform of $-1/\pi t$. We can therefore write the inverse Fourier transform of equation (A5) as:

$$s_G(t) = s(t) * \left[a\delta(t) - \frac{b}{\pi t}\right] = as(t) + b\mathrm{HT}[s(t)], \tag{A6}$$

where the asterisk $*$ denotes convolution and HT denotes Hilbert transform.

Equation (A6) is the result of starting our algorithm with an incorrect initial guess, and then imposing Hermitian symmetry on $S_G(f)$: we obtain a wavelet $s_G(t)$ which consists of a scaled version of the original wavelet $s(t)$ *plus* a scaled version of the Hilbert transform of $s(t)$. Since the Hilbert transform represents a convolution with an infinitely long operator, $s_G(t)$ is non-causal unless $b = 0$. That is, $s_G(t)$ will be non-causal unless $\theta = n\pi$, where n is an integer. If n is zero or even, $s_G(t)$ is a scaled version of $s(t)$ and has the same polarity; if n is odd the polarity of $s_G(t)$ is opposite to that of $s(t)$.

APPENDIX B
SOLUTION OF THE EQUATIONS IN THE TIME DOMAIN

We can reduce the problem to the solution of the two simultaneous equations (34) and (2):

$$s'(t) = s(t) * r(t) \tag{B1}$$

$$s'(t) = \alpha s(t/\alpha), \tag{B2}$$

in which $r(t)$ has been obtained from the data as described in section 3. Normally, we would use data which have been sampled at discrete time intervals. These two equations can thus be expressed in the z-domain as follows

$$S'(z) = S(z) \cdot \frac{R}{2} \cdot (z), \tag{B3}$$

$$S'(z^\alpha) = \alpha S(z), \tag{B4}$$

where the z-transform is defined as

$$S(z) = \sum_{t=-\infty}^{\infty} s_t z^t. \tag{B5}$$

If α is not an integer, equation (B4) indicates that we can find values of $S'(z)$ in between the sample points. This does not present any difficulty; we can simply interpolate or extrapolate to find values at the desired times.

The method we develop to find the coefficients s_t for different integer values of t is simply to equate the coefficients of z^t on opposite sides of equation (B3).

We recall from section 3 that we need two physical properties of $s(t)$ to constrain our solution; namely, that $s(t)$ is *real* and *causal*. By avoiding the transform to the frequency domain we avoid any introduction of *complex* numbers and operate entirely with *real* numbers. The *causality* constraint is simply the following:

$$s_t = 0 \quad \text{for } t \leq 0,$$

$$s'_t = 0 \quad \text{for } t < 0.$$

It follows that r_t is also causal if $s(t)$ is constrained to be minimum-phase hence

$$r_t = 0 \quad \text{for } t \leq 0.$$

We can rewrite equations (B3) and (B4) as follows:

$$(s'_0 + s'_1 z + s'_2 z^2 + \cdots) = (s_0 + s_1 z + s_2 z^2 + \cdots)(r_0 + r_1 z + r_2 z^2 + \cdots) \tag{B6}$$

$$s'_{\alpha n} = \alpha s_n, \tag{B7}$$

and we solve them iteratively in the following way:

(1) We guess s_1 (which is real). The effect of this guess being incorrect is simply to apply an unknown scale factor to the whole wavelet. This is unavoidable, but of trivial importance.

(2) Equate coefficients of z:

$s'_1 = s_1 r_0$.

(3) Use the scaling law, equation (B7) to give

$s'_\alpha = \alpha s_1$.

(4) Interpolate or extrapolate to find s'_2 (from s'_0, s'_1, s'_α).

(5) Equate coefficients of z^2:

$s'_2 = s_2 r_0 + s_1 r_1$. Hence s_2.

(6) Use equation (B7). Hence $s'_{2\alpha}$.

(7) Interpolate to find s'_3.

(8) We continue using the following general steps:

(a) $$s_n = \frac{s'_n - \sum_{i=1}^{n-1} s_i r_{n-i+1}}{r_0}$$

(b) $s'_{\alpha n} = \alpha s_n$

(c) Interpolate for s'_{n+1}

(d) Increase n by 1 and go back to (a).

Each loop in this iteration generates a further coefficient in the series s_t.

This scheme is conceptually very simple. It is also attractive compared with the frequency-domain because it avoids the trial-and-error approach which is required to find the causal source wavelet. There is, however, one big problem with this scheme: every coefficient of $S(z)$ is calculated from the expression in step 8(a) above, and appears to be sensitive to errors r_0. As each new coefficient is calculated it is required in the recursive computation of subsequent coefficients. Errors which may be small for the early coefficients will propagate and accumulate.

We have not tested this scheme for numerical stability, but because of the recursive nature of the calculation, we believe it may be unstable.

APPENDIX C

The energy in the elastic radiation is given by

$$E_E = 4\pi r^2 \int_0^\infty \dot{u}(\tau)p(\tau)\,d\tau, \tag{C1}$$

where $\dot{u}(t)$ is the particle velocity function, $p(t)$ is the pressure function ($p(\tau) = \rho c\dot{u}(\tau)$ in the far field), and $\tau = t - (r - a)/c$. Substituting for $\dot{u}(\tau)$ from equation (15) we find

$$E_E = 4\pi a^2 \rho c \int_0^\infty f^2(\tau/a)\,d\tau. \tag{C2}$$

If we now put $\eta = \tau/a$ (scaled time) we find

$$E_E = 4\pi a^3 \rho c \int_0^\infty f^2(\eta)\,d\eta. \tag{C3}$$

But we know from equations (6), (7), and (10) that the energy contained in the elastic radiation is given by

$$E_E = \frac{4\pi a^3 \beta k_2}{3(1-\beta)}. \tag{C4}$$

Therefore, equating these last two equations for E_E, we find

$$\int_0^\infty f^2(\eta)\,d\eta = \frac{\beta k_2}{3(1-\beta)\rho c}. \tag{C5}$$

In this last equation we see that $f(\eta)$ is a function of constants which depend on the medium and type of explosive only. Thus f is inherently a function of these two things only and is independent of the mass of the explosive.

APPENDIX D (AFTER R. CALVERT)

An elegant solution to the three basic equations (2), (4) and (5) has been suggested by R. Calvert. An outline is presented below.
In the frequency domain the equations are

$$X(f) = S(f)G(f), \tag{D1}$$

$$X'(f) = S'(f)G(f), \tag{D2}$$

$$S'(f) = \alpha^2 S(\alpha f). \tag{D3}$$

As before, a ratio function $R(f)$ is required. To ensure stability in the presence of noise a Wiener least squares estimate for $r(t)$ can be obtained

from the relationship

$$x'(t) = r(t) * x(t). \tag{35}$$

Fourier transformation of $r(t)$ then yields $R(f)$.
(D2) can now be written as

$$R(f)X(f) = S'(f)G(f). \tag{D4}$$

Taking logarithms, equations (D1), (D3), and (D4) become:

$$\ln X(f) = \ln S(f) + \ln G(f), \tag{D5}$$

$$\ln R(f) + \ln X(f) = \ln S'(f) + \ln G(f), \tag{D6}$$

$$\ln S'(f) = 2 \ln \alpha + \ln S(\alpha f). \tag{D7}$$

Subtracting (D5) from (D6) and substituting for $\ln S'(f)$ from (D7) yields

$$\ln R(f) - 2 \ln \alpha = \ln S(\alpha f) - \ln S(f). \tag{D8}$$

Changing the independent variable to $f' = \ln (f)$, this becomes

$$\ln R(f') - 2 \ln \alpha = \ln S(f' + \ln \alpha) - \ln S(f'),$$

which can be written in the convolutional form

$$\ln R(f') - 2 \ln \alpha = \ln S(f') * [\delta(f' + \ln \alpha) - \delta(f')]. \tag{D9}$$

The only unknown in equation (D9) is the function $\ln S(f')$. A least squares estimate of this can be obtained using the Wiener-Levinson algorithm on the real and imaginary parts of expression (D9) separately. It should be noted that the imaginary part of a complex logarithm is a phase function which must be "unwrapped" (Schafer 1969) to eliminate discontinuities.

Finally, the independent variable is converted back to $f = \exp (f')$ to yield the function $\ln S(f)$ whence exponentiation and inverse Fourier transformation leads to an estimate of the wavelet $s(t)$.

Although this method has not been tried in a full blown program, preliminary experiments suggest that it may be very sensitive to inaccurate estimates of the parameter α.

References

BERKHOUT A.J. 1970, Minimum phase in sampled signal theory, Ph.D. Thesis, Koninklijke Shell Exploration and Production Laboratory, Rijswijk, Netherlands.

BLAKE, F.G. 1952, Spherical wave propagation in solid media, Journal of the Acoustical Society of America 24, 211–215.

BRACEWELL R. 1965, The Fourier transform and its applications, McGraw-Hill, New York.

FRASIER C.W. and NORTH R.G. 1978, Evidence for ω-cube scaling from amplitudes and

periods of the Rat Island sequence (1965), Bulletin of the Seismological Society of America 68, 265–282.

NOOTEBOOM J.J. 1978, Signature and amplitude of linear gun arrays, Geophysical Prospecting 26, 194–201.

O'BRIEN P.N.S. 1969, Some experiments concerning the primary seismic pulse, Geophysical Prospecting 17, 511.

RICE R.B. 1962, Inverse convolution filters, Geophysics 27, 4–18.

RICKER N. 1940, The form and nature of seismic waves and the structure of seismograms, Geophysics 5, 348–366.

ROBINSON E.A. 1957, Predictive decomposition of seismic traces, Geophysics 22, 767–778.

ROBINSON E.A. 1967, Statistical communication and detection with special reference to digital data processing of radar and seismic signals, Griffin, London.

ROBINSON E.A., TREITEL S. et al. 1973, The Robinson-Treitel Reader, A collection of papers compiled by Seismograph Service Corporation, P.O. Box 1590, Tulsa, Oklahoma 74102, U.S.A.

SCHAFER R.W. 1969, Echo removal by discrete generalised linear filtering, Research Lab. of Electronics, MIT, Tech. Report 466.

SHARPE J.A. 1942, The production of elastic waves by explosion pressures, (1), Geophysics 7, 144–154.

SMITH S.G. 1975, Measurement of air gun waveforms, Geophysical Journal of the Royal Astronomical Society 42, 273–280.

LEVINSON N. 1947, The Wiener rms error criterion in filter design and prediction, Appendix B of Wiener, N. 1947, Extrapolation, Interpolation and Smoothing of Stationary Time Series, Wiley, New York.

ZIOLKOWSKI A.M. 1970, A method for calculating the output pressure waveform from an air gun, Geophysical Journal of the Royal Astronomical Society 21, 137–161.

ZIOLKOWSKI A.M. 1971, Design of a marine seismic reflection profiling system using air guns as a sound source, Geophysical Journal of the Royal Astronomical Society 23, 499–530.

ZIOLKOWSKI A.M. and LERWILL W.E. 1979, A simple approach to high resolution seismic profiling for coal, Geophysical Prospecting 27, 360–393.